0026-895X/08/7403-605–613$20.00
MOLECULAR PHARMACOLOGY
Copyright © 2008 The American Society for Pharmacology and Experimental Therapeutics
Mol Pharmacol 74:605–613, 2008

Vol. 74, No. 3
48017/3373245
Printed in U.S.A.

Ligand-Receptor Interactions at the Parathyroid Hormone Receptors: Subtype Binding Selectivity Is Mediated via an Interaction between Residue 23 on the Ligand and Residue 41 on the Receptor

Rosalind Mann, Mark J. Wigglesworth, and Dan Donnelly

Institute of Membrane & Systems Biology, LIGHT Laboratories, Faculty of Biological Sciences, University of Leeds, Leeds, United Kingdom (R.M., D.D.); and Screening and Compound Profiling, GlaxoSmithKline, New Frontiers Science Park North, Harlow, United Kingdom (M.J.W.)

Received April 17, 2008; accepted June 6, 2008

ABSTRACT

Parathyroid hormone (PTH) and parathyroid hormone-related peptide (PTHrP) bind and activate the PTH/PTHrP receptor (PTH-1R). However, while the related receptor PTH-2R responds potently to PTH, it is not activated by PTHrP. Two hormone sites are known to be responsible for these different potencies. First, the absence of efficacy for PTHrP at PTH-2R is due to the presence of His-5 in PTHrP (Ile-5 in PTH), which interacts with the receptor's juxtamembrane domain. Second, PTHrP has lower affinity than PTH for PTH-2R because of the presence of Phe-23 (Trp-23 in PTH), which interacts with the receptor's N-terminal extracellular domain. We used these different receptor subtype properties to demonstrate that residue 41 in PTH-1R, when either the native Leu or substituted by Ile or Met, can accommodate either Phe or Trp at position 23 of the ligand. However, when Leu-41 is substituted by a smaller side chain, either Ala or Val (its equivalent residue in PTH-2R), the receptor becomes highly selective for those peptide ligands with Trp-23. Hence, despite the conservative nature of the substitutions found in the native ligands (Phe for Trp) and receptors (Leu for Val), they nevertheless enable a significant degree of selectivity to be achieved. Analysis of this functionally important ligand-receptor contact, within the context of the recent X-ray structure of the peptide-bound PTH-1R N domain, reveals the nature of the selectivity filter and how it is by-passed in PTH-1R.

Parathyroid hormone (PTH) and parathyroid hormone-related peptide (PTHrP) mediate many of their physiological effects via the same receptor, PTH-1R (Lanske et al., 1996). Although PTH has 84 residues and PTHrP has 141 residues, the biological effects they mediate via PTH-1R can be replicated by synthetic peptides equivalent to the first 34 amino acids of each peptide (e.g., Segre et al., 1979). These shorter analogs bind and activate PTH-1R in an manner analogous to that of the "two-site model" seen at other related family B G protein-coupled receptors (GPCRs) (Bergwitz et al., 1996; López de Maturana et al., 2003; Castro et al., 2005). In this model, the ligand's C-terminal region interacts with the receptor's N-terminal extracellular domain (N domain) to generate affinity. This first interaction positions the N-terminal region of the peptide such that it activates the receptor via a second interaction with the receptor's juxtamembrane "core" domain, comprising the transmembrane helices and connecting loops. The nature of the first interaction has been investigated via a number of mutagenic and cross-linking studies (Mannstadt et al., 1998; Gensure et al., 2001; Pham and Sexton, 2004) and more recently has been the focus of several structural studies that defined the structures of the peptide-bound N domains of the receptors for corticotropin-releasing factor, pituitary adenylyl cyclase-activating polypeptide, glucose-dependent insulinotropic peptide (GIP), glucagon-like peptide-1 (GLP-1) and, very recently, PTH itself (Grace et al., 2004, 2007; Parthier et al., 2007; Sun et al., 2007; Pioszak and Xu, 2008; Runge et al., 2008).

In addition to its actions at PTH-1R, PTH is also a potent

This work was funded by the Biotechnology and Biological Sciences Research Council and GlaxoSmithKline.
Article, publication date, and citation information can be found at http://molpharm.aspetjournals.org.
doi:10.1124/mol.108.048017.

ABBREVIATIONS: PTH, parathyroid hormone; PTHrP, parathyroid hormone-related peptide; GPCR, G protein-coupled receptor; N domain, N-terminal extracellular domain; GIP, glucose-dependent insulinotropic peptide; GLP-1, glucagon-like peptide-1; PTH-1R, PTH/PTHrP receptor; PTH-2R, parathyroid hormone-2 receptor; HEK, human embryonic kidney; PBS, phosphate-buffered saline; PTHrP(1–36), Tyr36-PTHrP(1–36); Trp23-PTHrP(1–36), Trp23,Tyr36-PTHrP(1–36); ^{25}I-rPTH(1–34), ^{125}I-[Nle^{8,21},Tyr^{34}]rPTH(1–34)NH_2; MBS, membrane binding solution.

agonist at PTH-2R, a related receptor with approximately 50% sequence identity to PTH-1R (Usdin et al., 1995). However, despite the high potency of PTH, PTHrP binds to PTH-2R with more than 100-fold lower affinity and, furthermore, has virtually no biological efficacy. Hence, PTH acts as a potent agonist at both receptors but PTHrP acts as a high-affinity agonist at PTH-1R and has relatively low affinity and almost no detectable efficacy at the PTH2R.

An elegant study by Gardella et al. (1996) determined that, despite sharing only 11 of their first 34 residues, the components of the hormones responsible for their different properties at PTH-2R are located at only two sites. First, Gardella et al. (1996) demonstrated that His-5* (ligand residues are distinguished from receptor residues by an asterisk after the residue number) in PTHrP is the residue responsible for its absence of biological efficacy and that, when substituted by Ile (the equivalent residue in PTH), its biological activity is restored. According to the two site model for family B GPCR peptide-ligand interactions, the interaction site for residue 5* in PTH and PTHrP would be expected to be within the J domain; indeed, two reciprocal studies have demonstrated this to be the case (Bergwitz et al., 1997; Turner et al., 1998). The second site demonstrated by Gardella et al. (1996) to be responsible for PTHrP's impaired response at PTH-2R is residue 23*, which is Phe in PTHrP but Trp in PTH. Rather than influencing peptide efficacy, as for residue 5, the presence of Phe at residue 23* reduces the peptide's affinity at PTH-2R by approximately 70-fold relative to the equivalent peptide with Trp-23*, despite the relatively similar nature of these two aromatic amino acid side chains. The two-site model for peptide-ligand interaction would predict that residue 23* interacts with the receptor's N domain and, once again, this has been demonstrated (Mannstadt et al., 1998; Gensure et al., 2001; Dean et al., 2006; Pioszak and Xu, 2008).

Taken together, the information from the studies reviewed above suggests that PTH-2R contains a selectivity filter within its N domain that selects against peptide ligands containing Phe at position 23* but not against those containing Trp; we will refer to this as the "Trp23/Phe23 selectivity filter." To demonstrate this, we hypothesized that this selectivity filter could be moved from PTH-2R into PTH-1R with the result of increasing the sensitivity of PTH-1R to the nature of the residue at position 23* of the ligand. Starting with a chimeric receptor to demonstrate the proof of principle, our ultimate objective was to identify a specific residue in the N domain that confers the Trp23/Phe23 selectivity. The very recent publication of the X-ray structure of PTH bound to the N domain of PTH-1R allowed us to interpret our data in this structural context and to explain the nature of the peptide selectivity at PTH receptors.

Materials and Methods

Constructs. The full-length cDNA of human PTH-1R and PTH-2R (gift from GlaxoSmithKline) were individually ligated into the multiple cloning site of pcDNA3 (Invitrogen, Paisley, UK) using the restriction sites for BamHI and NotI (for PTH-1R) and HindIII and XhoI (for PTH-2R). Two cross-linking studies have determined that a benzoylphenylalanine substituted at position 23* of PTHrP can be covalently cross-linked to the distal region of the N domain, more specifically either to residues 23 to 40 in rat PTH-1R or 33 to 63 in human PTH-1R (Mannstadt et al., 1998; Gensure et al., 2001). Hence, a receptor chimera PTH1R-NT2, encoding a receptor with residues 1 to 43 from PTH-2R and residues 44 to 593 of PTH-1R, was constructed by introducing a unique AflII restriction site into both the PTH-1R and PTH-2R cDNA at codons 42/43 using QuikChange site-directed mutagenesis (Stratagene, La Jolla, CA). As a result, His-42 and Arg-43 in PTH-1R were mutated to Leu and Lys, respectively, the corresponding residues from PTH-2R. These two pcDNA3-based constructs were then cleaved with AflII, within the cDNA, and also with XbaI, which cuts in the 3′ polylinker region. The appropriate AflII-XbaI DNA fragments were gel-purified and ligated to yield the PTH1R-NT2 chimera cDNA. All enzymes were purchased from New England Biolabs (Hitchin, UK). All other mutated receptors were generated using QuikChange site-directed mutagenesis and confirmed by DNA sequencing. These various pcDNA3 constructs were used to express the wild type, PTH1R-NT2 chimera, and mutant PTH receptors in human embryonic kidney (HEK)-293 cells.

Cell Culture. The HEK-293 cells were cultured in Dulbecco's modified Eagle's medium (Sigma, Poole, UK) supplemented with 10% fetal calf serum (Lonza Wokingham Ltd., Wokingham, Berkshire, UK) and containing 2 mM L-glutamine, 100 U/ml penicillin, and 100 μg/ml streptomycin (Invitrogen, Paisley, UK). Cells were transfected with pcDNA3 containing the cDNA encoding the receptors, using the SuperFect Transfection Reagent (QIAGEN Ltd., Crawley, UK), and stable clones were selected with G418 antibiotic (Geneticin; Invitrogen) as follows. Cells were seeded into a 25-cm^2 flask containing 10 ml of media and transfected when they reached 50 to 80% confluence. To do this, 20 μl of SuperFect was mixed with a DNA solution consisting of 5 μg of plasmid DNA in 150 μl of Dulbecco's modified Eagle's medium. The DNA was incubated with the reagent for 10 min at room temperature, after which 1 ml of media was added and mixed gently. The cells were washed once with sterile PBS (137 mM NaCl, 10 mM phosphate, and 2.7 mM KCl, pH 7.4) before the transfection mixture was added and incubated for 3 h at 37°C. The cells were then washed three times with PBS before the addition of fresh media. Three days later, the supernatant was removed and the cells were washed with PBS before fresh media was added. Selection of transfected cells was achieved by addition of 800 μg/ml G418. The medium, containing G148, was replaced every 3 days until individual colonies were clearly visible. Approximately 10 to 20 individual colonies were detached from the flask using trypsin, seeded in a fresh plate, and grown to confluence.

Peptides. PTH(1–34) and Tyr36-PTHrP(1–36) [called PTHrP(1–36) throughout the text] were from Bachem (Saffron Walden, UK). Phe23-PTH(1–34) and Trp23,Tyr36-PTHrP(1–36) [called Trp23-PTHrP(1–36) throughout the text] were custom-synthesized by Cambridge Research Biochemicals (Cambridge, UK) by solid-phase synthesis on an Advanced ChemTech peptide synthesizer. After high-performance liquid chromatography purification and analysis, alongside matrix-assisted laser desorption ionization/time of flight mass spectrometry, 10 mg of >95% pure peptide was supplied. The radioligand ^{125}I-[Nle^{8,21},Tyr^{34}]rPTH(1–34)NH$_2$ [called ^{125}I-rPTH(1–34) throughout the text] was from PerkinElmer Life and Analytical Sciences (Waltham, MA).

Ligand Binding to Whole Cells. Radioligand binding was carried out using cells grown in 24-well plates (adapted from Gardella et al., 1996). Each well contained a final volume of 300 μl and contained 50 pM (~60,000 cpm) ^{125}I-rPTH(1–34) and various concentrations of an unlabeled competitor ligand, all diluted in whole-cell binding buffer (50 mM Tris-HCl, pH 7.7, 100 mM NaCl, 5 mM KCl, 2 mM $CaCl_2$, 5% heat-inactivated horse serum, and 0.5% heat-inactivated fetal bovine serum). Binding assays were incubated at room temperature for 2 h before being washed three times with 0.5 ml of whole-cell binding buffer. The cells were then lysed by addition of 0.5 ml of 5 M NaOH, and the lysate was measured for radioactivity in a γ counter (RiaStar 5405 counter; PerkinElmer Life and Analytical Sciences, Waltham, MA). Total radioligand bound was <10% and nonspecific binding was ~1% of total counts added. PTH-2R could only be detected in whole cell binding experiments.

Ligand Binding to Membranes. The method was adapted from Hoare and Usdin (1999). HEK-293 cells, cultured to confluence on five 160-cm^2 Petri dishes (precoated with poly-D-lysine), were washed with PBS, followed by the addition of 15 ml of ice-cold, sterile, double-distilled water to induce cell lysis. After 5 min incubation on ice, the ruptured cells were thoroughly washed with ice-cold PBS before being scraped from the plates and pelleted by centrifugation in a bench-top centrifuge (13,000*g* for 30 min). The crude membrane pellet was resuspended in 1 ml of membrane binding solution (MBS; 20 mM HEPES, pH 7.5, 100 mM $NaCl_2$, 1 mM EDTA, 3 mM $MgSO_4$, and 50 mg/l bacitracin) and forced through a 23-gauge needle after which 0.1-ml aliquots were snap-frozen in liquid nitrogen and stored at −70°C. Membranes were slowly thawed on ice before diluting to a concentration that gave total radioligand binding of <10% of the total counts added. In a reaction volume of 200 μl, 75 pM (~60,000 cpm) ^{125}I-rPTH(1–34), various concentrations of an unlabeled competitor ligand and HEK-293 membranes expressing the receptor of interest were combined, all diluted in MBS supplemented with 0.3% nonfat milk powder. Assays were carried out in polypropylene "V"-bottomed 96-well plates (Nalge Nunc International, Rochester, NY) for 1 h. MultiScreen 96-well filtration plates (polyvinylidene fluoride filters, 0.45-μm pore size; Millipore, Bedford, MA) were presoaked in a 1% nonfat milk powder/PBS solution for 30 min. After the incubation, membrane-associated radioligand was harvested by transferring the assay mixture to the filtration plate housed in a vacuum manifold. The wells of the assay plate were washed with 0.2 ml of MBS, which was transferred to the filtration plate. The wells were then washed three times with 0.2 ml of MBS before harvesting the filter discs. Filter-bound radioactivity was measured in a γ counter.

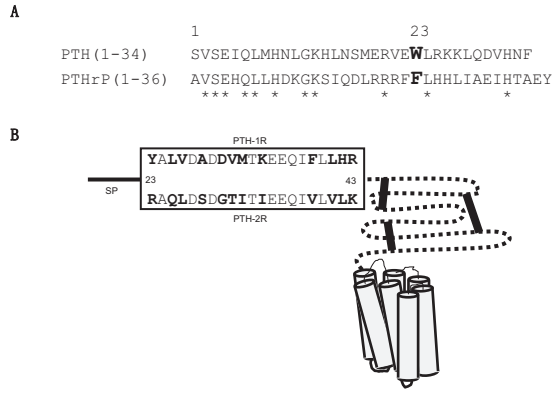

Fig. 1. A, sequence alignment of PTH(1–34) and PTHrP(1–36), the peptides used in this study. Note that residue Ile-36 of PTHrP(1–36) has been substituted by Tyr. Conserved residues are highlighted with the asterisks (*), and the residues at position 23 are highlighted with a large/bold font. B, a diagram of the PTH receptors showing the aligned sequences of both PTH-1R and PTH-2R between residues 23 and 43. This region immediately follows the signal peptide (SP) and therefore represents the extreme N-terminal region of the mature receptors. The dotted line represents the remainder of the N domain, which typifies all family B GPCRs, with the three solid lines representing the three disulfide bonds. The transmembrane core domain is represented by the bundle of seven cylinders.

Data Analysis. For each individual competition binding experiment, counts were normalized to the maximal specific binding within each data set. IC_{50} values were calculated with a single-site binding model fitted using nonlinear regression with the aid of Prism 3.0 software (GraphPad Software, San Diego, CA). Values in the tables represent the mean with S.E.M. calculated from the individual pIC_{50} values (−Log IC_{50}) from at least three independent experiments. Binding curves in the figures represent pooled data from three independent experiments, where each point is the mean of the normalized values with interexperimental S.E.M. displayed as error bars.

Molecular Modeling. The X-ray structure of the PTH-1R N domain with bound PTH (Pioszak and Xu, 2008; Protein Data Bank code 3C4M) was published during the writing of this manuscript. To use this new information to interpret the mutagenesis data described in this article, in silico mutagenesis of this X-ray structure was carried out using the "Mutate Monomers" tool within the "Biopolymer" module of SYBYL ver. 6.3 (Tripos Associates, St. Louis, MO). The structure and nine models accounted for all combinations of the receptor residue 41 as Leu, Val, Ile, Met, or Ala with the PTH peptide residue 23* as Trp or Phe. The in silico mutagenesis of Trp-23* to Phe resulted in a conformation in which the benzoyl ring lay in the same plane as the original indole ring of Trp-23*. All

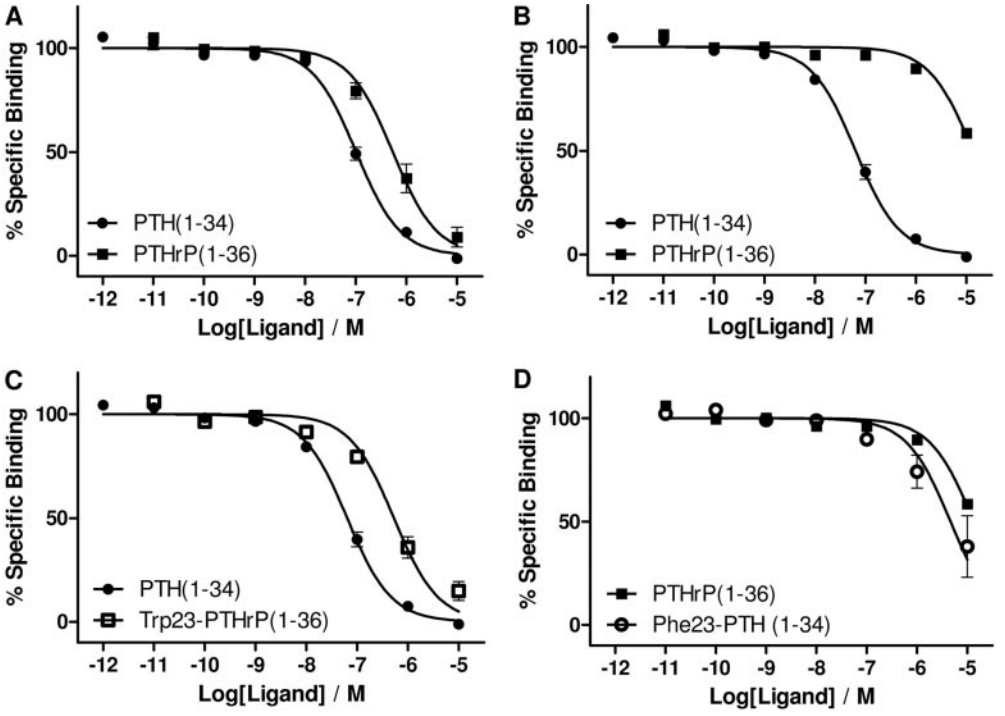

Fig. 2. Intact HEK-293 cells expressing either PTH-1R (A) or PTH-2R (B–D) were used in competition binding assays using ^{125}I-rPTH(1–34) as the tracer and one of four unlabeled peptide ligands: PTH(1–34) (●); PTHrP(1–36) (■); Phe23-PTH(1–34) (○); and Trp23-PTHrP(1–36) (□). Each panel represents pooled data from three independent experiments. Using whole cells, the mean pIC_{50} values at PTH-1R were 7.00 ± 0.10 for PTH(1–34) and 6.27 ± 0.26 for PTHrP(1–36), whereas at PTH-2R, they were 7.20 ± 0.11 for PTH(1–34), 4.87 ± 0.04 for PTHrP(1–36), 5.34 ± 0.55 for Phe23-PTH(1–34), and 6.27 ± 0.20 for Trp23-PTHrP(1–36). The small selectivity of PTH(1–34) over PTHrP(1–36) observed at PTH-1R (A) is significantly enhanced at PTH-2R (B). This increase in peptide selectivity is determined by the nature of residue 23, which is Trp in PTH(1–34) and Phe in PTHrP(1–36) (C and D).

allowed side-chain rotamers of residue 41 were then explored by adjusting the χ dihedral angles within the ranges permitted for each residue type when located in the center of an α-helix (Penel and Doig, 2001). *Gauche*(+) refers to $\chi \approx -60°$, *trans* refers to $\chi \approx 180°$, and *gauche*(−) refers to $\chi \approx +60°$, where $\chi 1$ was measured from the main chain nitrogen atom to γ of Leu, $\gamma 1$ of Ile, and $\gamma 2$ of Val, whereas $\chi 2$ was measured from the Cα atom to δ of Ile and $\delta 1$ of Leu. Rotamer combinations that resulted in serious steric interference with other parts of the model were rejected, whereas those that formed stabilizing contacts with the ligand were prioritized. Where no side chain-to-side chain interaction between residue 41 and 23* could be obtained through altering the rotamer of residue 41, modest adjustment of the rotamer of residue 23* was explored within ± 15° of the $\chi 1$ and $\chi 2$ values found in the crystal structure. Once the particular side-chain conformations for each mutant/ligand combination had been selected, each resultant model was subjected to energy minimization (2000 steps of conjugate gradients using the Tripos force field). Models were further analyzed visually using SYBYL 6.3 to measure atom-atom distances, dihedral angles and to analyze the potential mechanism of the Trp23/Phe23 selectivity.

Results

Fig. 1A shows the sequence of PTH(1–34) and PTHrP(1–36) with position 23* highlighted in bold. The affinities of these peptides at PTH-1R and PTH-2R, expressed in whole HEK-293 cells, were estimated using competition binding assays (Fig. 2, A and B). At PTH-1R, the peptides displayed a less than 6-fold difference in IC_{50}, whereas at PTH-2R, the difference was greater than 200-fold. Two additional peptides, Phe23-PTH(1–34) and Trp23-PTHrP(1–36), were used in this study by substituting position 23* of PTH(1–34) and PTHrP(1–36), respectively. The effect of these substitutions, in either peptide, was to reduce the 214-fold selectivity at PTH-2R (Fig. 2B) to less than 10-fold (Fig. 2, C and D).

To locate the site in PTH-2R responsible for the improved affinity of the peptide ligands with Trp-23* over those with Phe-23*, a chimeric receptor, PTH1R-NT2, was created with residues 1 to 43 from PTH-2R and residues 44 to 593 of PTH-1R (Fig. 1B). PTH1R-NT2 and PTH-1R were expressed in HEK-293 cells from which membrane preparations were analyzed using competition binding assays. The chimeric receptor had a 277-fold selectivity for PTH(1–34) over PTHrP(1–36) compared with only 16-fold at PTH-1R (Table 1; Fig. 3). Furthermore, compared with PTH-1R, the PTH1R-NT2 chimera displayed a greater selectivity of Phe23-PTH(1–34) relative to PTH(1–34) (108-fold compared with 11-fold) and also for PTHrP(1–36) relative to Trp23-PTHrP(1–36) (124-fold compared with 7-fold) (Table 1). The data demonstrated that the selectivity filter in PTH-2R had been moved to PTH-1R and that, given that the first 23 residues of the receptors are signal peptides, it lies within the first 21 residues of the mature receptor. No significant differences were observed in the activation properties of PTH1R-NT2 relative to PTH-1R, as measured using concentration-response curves to measure agonist-induced cAMP accumulation (data not shown). This was expected because large affinity changes at PTH-1R are known to result in only very modest potency changes (Gardella et al., 1996), possibly because of a large receptor reserve, thereby making functional assays of limited use relative to binding assays in this particular context.

The region of PTH-1R and PTH-2R made up of residues 23 to 43 differs at only 12 of the 21 sites. To identify the specific residue or residues responsible for the Trp23/Phe23 selectivity in the chimera, six site-directed double mutants of PTH-1R were prepared in which pairs of residues were replaced by their equivalents in PTH-2R. The double mutants were expressed in HEK-293 cells and, as before, membrane preparations were analyzed using competition binding assays (Table 2). Five of the double mutants displayed a selectivity between PTH(1–34) and PTHrP(1–36) of only 13- to 45-fold, compared with the 16-fold difference observed with PTH-1R. However, one double mutant, FL39/41VV, displayed a selectivity of >500-fold. Further single mutations at these two sites demonstrated that the increased selectivity was due not to the F39V mutation (27-fold) but to the L41V substitution (>900-fold) (Table 2).

TABLE 1

Binding properties of the chimeric receptor PTH1R-NT2 compared with wild type PTH-1R

Values represent mean pIC_{50} values ± S.E. for three independent competition binding assays using membrane preparations and four different unlabeled ligands with ^{125}I-rPTH(1–34) as the tracer. The values are compared using d1, d2, or d3 which represent the -fold change in mean IC_{50} values, where d1 compares PTHrP(1–36) relative to PTH(1–34), d2 compares Phe23-PTH(1–34) relative to PTH(1–34), and d3 compares PTHrP(1–36) relative to Trp23-PTHrP(1–36). d1, d2, and d3 values for PTH-2R from whole cell binding were 213, 72 and 25, respectively (from Figure 2), or 134, 28 and 71, respectively (from Gardella et al., 1996).

	PTH(1–34)	PTHrP(1–36)	d1	Phe23-PTH(1–34)	d2	Trp23-PTHrP(1–36)	d3
PTH-1R	8.02 ± 0.17	6.81 ± 0.29	16	6.99 ± 0.21	11	7.65 ± 0.15	7
PTH1R-NT2	8.45 ± 0.13	6.01 ± 0.05	277	6.42 ± 0.19	108	8.10 ± 0.25	124

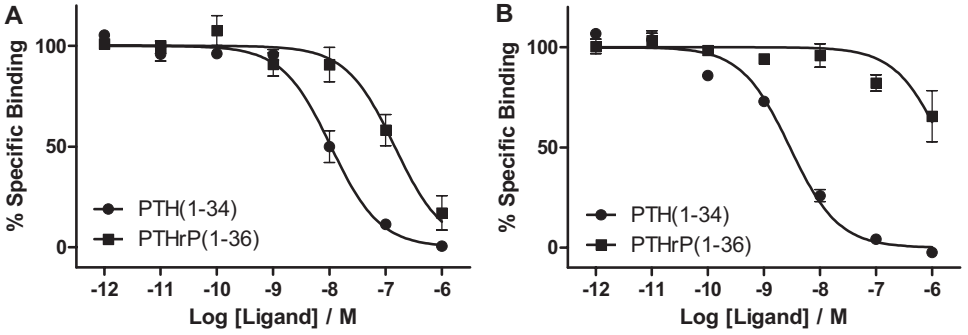

Fig. 3. Membrane preparations from HEK-293 cells, expressing either PTH-1R (A) or the chimera PTH1R-NT2 (B), were used in competition binding assays using ^{125}I-rPTH(1–34) as the tracer and two unlabeled peptide ligands: PTH(1–34) (●) and PTHrP(1–36) (■). Each panel represents pooled data from three independent experiments. The small 16-fold selectivity of PTH(1–34) over PTHrP(1–36) observed at PTH-1R (A) is significantly enhanced to 277-fold at PTH1R-NT2 (B). Full data for these and other peptides are shown in Table 1.

To further understand the nature of the PTH/PTHrP selectivity conferred by the Leu-to-Val change at residue 41, three additional mutations were made at this site in PTH-1R to create L41A, L41I, and L41M. The Leu-41 mutants were expressed in HEK-293 cells and, as before, membrane preparations were analyzed using competition binding assays using four unlabeled peptides (Table 3). Despite the conservative nature of the substitutions introduced at Leu-41, two distinct receptor phenotypes were observed. The first phenotype was represented by L41I and L41M, which resembled wild-type PTH-1R with modest PTH/PTHrP and Trp23/Phe23 selectivity. The second phenotype was represented by L41V and L41A, which displayed a much greater PTH/PTHrP and Trp23/Phe23 selectivity that closely resembled that observed for the chimeric PTH1R-NT2 and wild-type PTH2-R receptors. For example, Fig. 4 displays a comparison of the binding properties of PTH(1–34) and Phe23-PTH(1–34) at PTH-1R (Fig. 4A) and three mutant receptors (Fig. 4, B–D). The modest selectivity between the peptide ligands when residue 41 is Leu or Ile (Fig. 4, A and C) is greatly increased when residue 41 is Val or Ala (Fig. 4, B and D). Likewise, Fig. 5 displays a comparison of the binding properties of PTHrP(1–36) and Trp23-PTHrP(1–36) at PTH-1R (Fig. 5A) and three mutant receptors (Figs. 5, B–D). Once again, the modest selectivity between the peptide ligands when reside 41 is Leu or Ile (Fig. 5, A and C) is greatly increased when residue 41 is Val or Ala (Fig. 5, B and D).

In silico mutagenesis of the crystal structure of PTH bound to the N domain of PTH-1R was used to explore the mechanism of the Trp23/Phe23 selectivity filter. In the X-ray structure, the $\chi 1$ and $\chi 2$ conformation of Leu-41 is *trans*, *gauche*(−) rather than the more common *gauche*(+), *trans* rotamer, which would result in a steric clash with Trp-23*. However, when Trp-23* is substituted by Phe-23*, the *gauche*(+), *trans* combination resulted in no such steric interference with the ligand but rather enabled a van der Waals contact with Phe-23* that had not possible with the original *trans*, *gauche*(−) rotamer. For Val and Ile at position 41, the β-branch meant that only one conformation of $\chi 1$ was allowed, because a β carbon atom at approximately +60° is disfavored due to clashes with the main chain of the helix. Hence only the *gauche*(+) was possible for Val-41, whereas for Ile, the highly favored *gauche*(+), *trans* combination (Penel and Doig, 2001) resulted in steric clashes with Trp-23* (hence disallowed in the PTH-bound model) but was nevertheless the only rotamer able to form a stabilizing van der Waals contact with Phe-23*. On the other hand, the *gauche*(+), *gauche*(+) combination allowed a van der Waals interaction with Trp-23* but could not interact with Phe-23*. The Met-41 mutants were built with equivalent rotamers to the Leu such that the sulfur atom was positioned with topological equivalence to the particular δ of Leu-41 that contacted residue 23* ($\delta 2$ for Trp-23* and $\delta 1$ for Phe-23*). The choice of the Ala-41 model was trivial because it adopts only one conformation.

The effect of these in silico mutations and energy minimization on the local structure of the N domain was negligible, which was expected from the experimental data, which clearly showed that these mutations had no effect on PTH affinity, thereby demonstrating that the protein structure had not been unduly perturbed.

TABLE 2

Binding properties of mutant receptors compared with wild type PTH-1R

Values represent mean pIC_{50} values ± S.E. for three independent competition binding assays using two unlabeled ligands with ^{125}I-rPTH(1–34) as the tracer. The values are compared using d1, which represents the -fold change in the mean IC_{50} value of PTHrP(1–36) relative to PTH(1–34).

	PTH(1–34)	PTHrP(1–36)	d1
PTH-1R	8.02 ± 0.17	6.81 ± 0.29	16
YL23/25RQ	8.47 ± 0.24	6.83 ± 0.08	44
VA26/28LS	8.10 ± 0.06	6.86 ± 0.08	17
DV30/31GT	8.28 ± 0.16	6.63 ± 0.17	45
MK32/34II	8.15 ± 0.12	7.02 ± 0.09	13
FL39/41VV	8.46 ± 0.20	5.71 ± 0.14	558
HR42/43LK	8.14 ± 0.17	6.85 ± 0.34	20
F39V	7.97 ± 0.09	6.54 ± 0.19	27
L41V	8.40 ± 0.18	5.43 ± 0.02	935

Discussion

To locate the Trp23/Phe23 selectivity filter (Gardella et al., 1996; Fig. 2), we set out to move it from PTH-2R to PTH-1R with the expectation that the modified PTH-1R would display an increase in "Trp23/Phe23 selectivity." Previous work had demonstrated that position 23* binds to the receptor's N domain (Dean et al., 2006) and, moreover, can be cross-linked to either residues 23 to 40 in rat PTH-1R or 33 to 63 in human PTH-1R (Mannstadt et al., 1998; Gensure et al., 2001). We therefore started our search by substituting the first 21 residues of the mature PTH-1R (Y23-R43) with the equivalent residues in PTH-2R (R23-K43) (Fig. 1B) to yield a chimeric receptor called PTH1R-NT2. The chimera displayed a greatly increased Trp23/Phe23 selectivity (Fig. 3; Table 1), demonstrating that the selectivity filter had been successfully transferred and, moreover, that it was likely to be the result of one or more of the 12 residues in this region that differ between the two receptors.

The construction and analysis of six double mutants, followed by two further single mutations, identified the Leu-41-to-Val change as the only substitution responsible for the increased PTH/PTHrP selectivity (Table 2). Therefore, the

TABLE 3

Binding properties of PTH-1R mutated at residue Leu41 compared with wild type PTH-1R

Values represent mean pIC_{50} values ± S.E. for three independent competition binding assays using four different unlabeled ligands with ^{125}I-rPTH(1–34) as the tracer. The values are compared using d2 or d3, which represent the -fold change in mean IC_{50} values, where d2 compares Phe23-PTH(1–34) relative to PTH(1–34) and d3 compares PTHrP(1–36) relative to Trp23-PTHrP(1–36).

	PTH(1–34)	Phe23-PTH(1–34)	d2	PTHrP(1–36)	Trp23-PTHrP(1–36)	d3
PTH-1R	8.02 ± 0.17	6.99 ± 0.21	11	6.81 ± 0.29	7.65 ± 0.15	7
L41V	8.40 ± 0.18	6.38 ± 0.31	104	5.43 ± 0.02	7.96 ± 0.23	341
L41A	8.09 ± 0.12	5.24 ± 0.23	705	<5	7.07 ± 0.06	>100
L41I	7.91 ± 0.23	7.23 ± 0.20	5	7.12 ± 0.13	7.79 ± 0.04	5
L41M	8.03 ± 0.06	6.57 ± 0.24	29	6.54 ± 0.30	7.21 ± 0.13	5

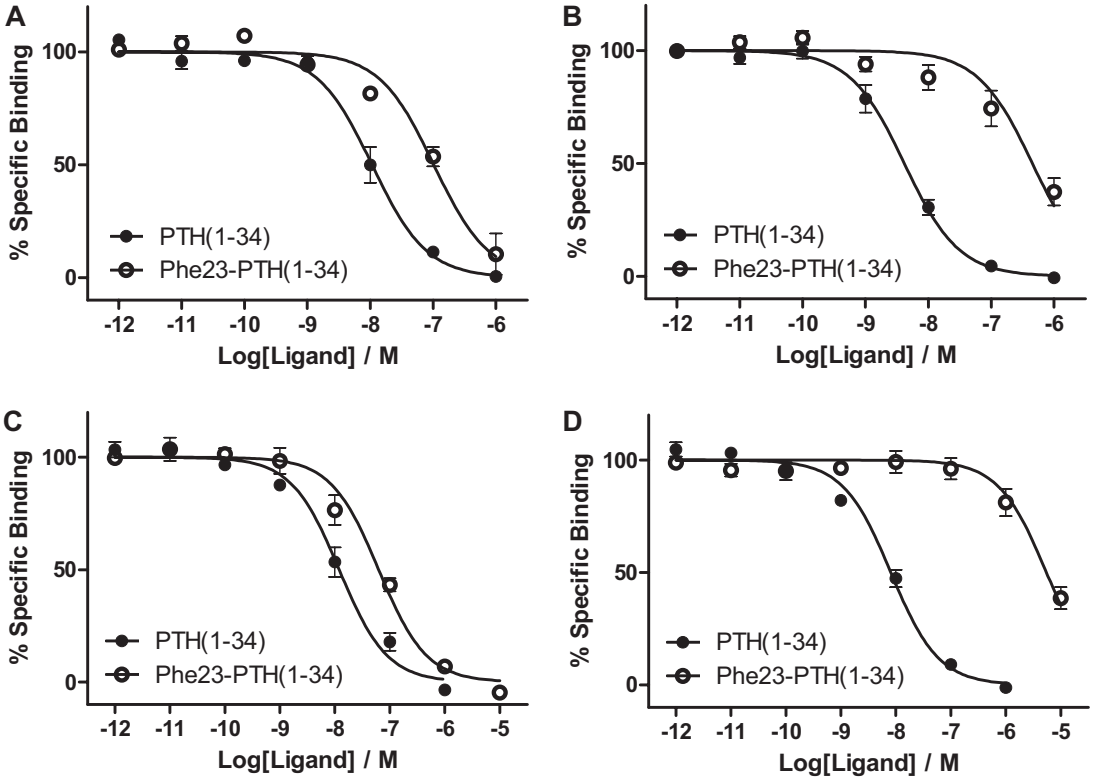

Fig. 4. Membrane preparations from HEK-293 cells expressing either PTH-1R (A), L41V (B), L41I (C), or L41A (D) were used in competition binding assays using ^{125}I-rPTH(1–34) as the tracer and two unlabeled peptide ligands: PTH(1–34) (●) and Phe23-PTH(1–34) (○). Each panel represents pooled data from three independent experiments. The small 11-fold selectivity of PTH(1–34) over Phe23-PTH(1–34) observed at PTH-1R (A) is significantly enhanced to 104-fold at L41V (B), despite there being only a 5-fold selectivity at L41I (C). Selectivity is increased to 705-fold in L41A (D). Full data for these and other peptides are shown in Table 3.

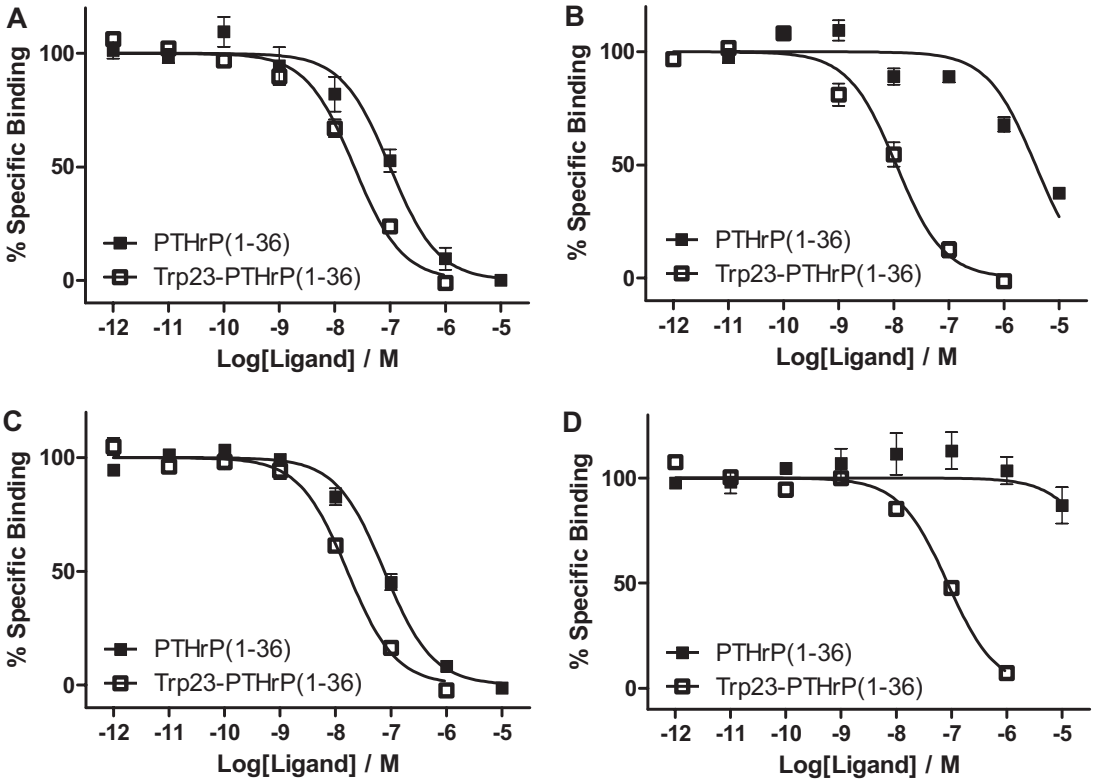

Fig. 5. Membrane preparations from HEK-293 cells expressing either PTH-1R (A), L41V (B), L41I (C), or L41A (D) were used in competition binding assays using ^{125}I-rPTH(1–34) as the tracer and two unlabeled peptide ligands: PTHrP(1–36) (■) and Trp23-PTHrP(1–36) (□). Each panel represents pooled data from three independent experiments. The small 7-fold selectivity of Trp23-PTHrP(1–36) over PTHrP(1–36) observed at PTH-1R (A) is significantly enhanced to 341-fold at L41V (B), despite there being only a 5-fold selectivity at L41I (C). Full data for these and other peptides are shown in Table 3.

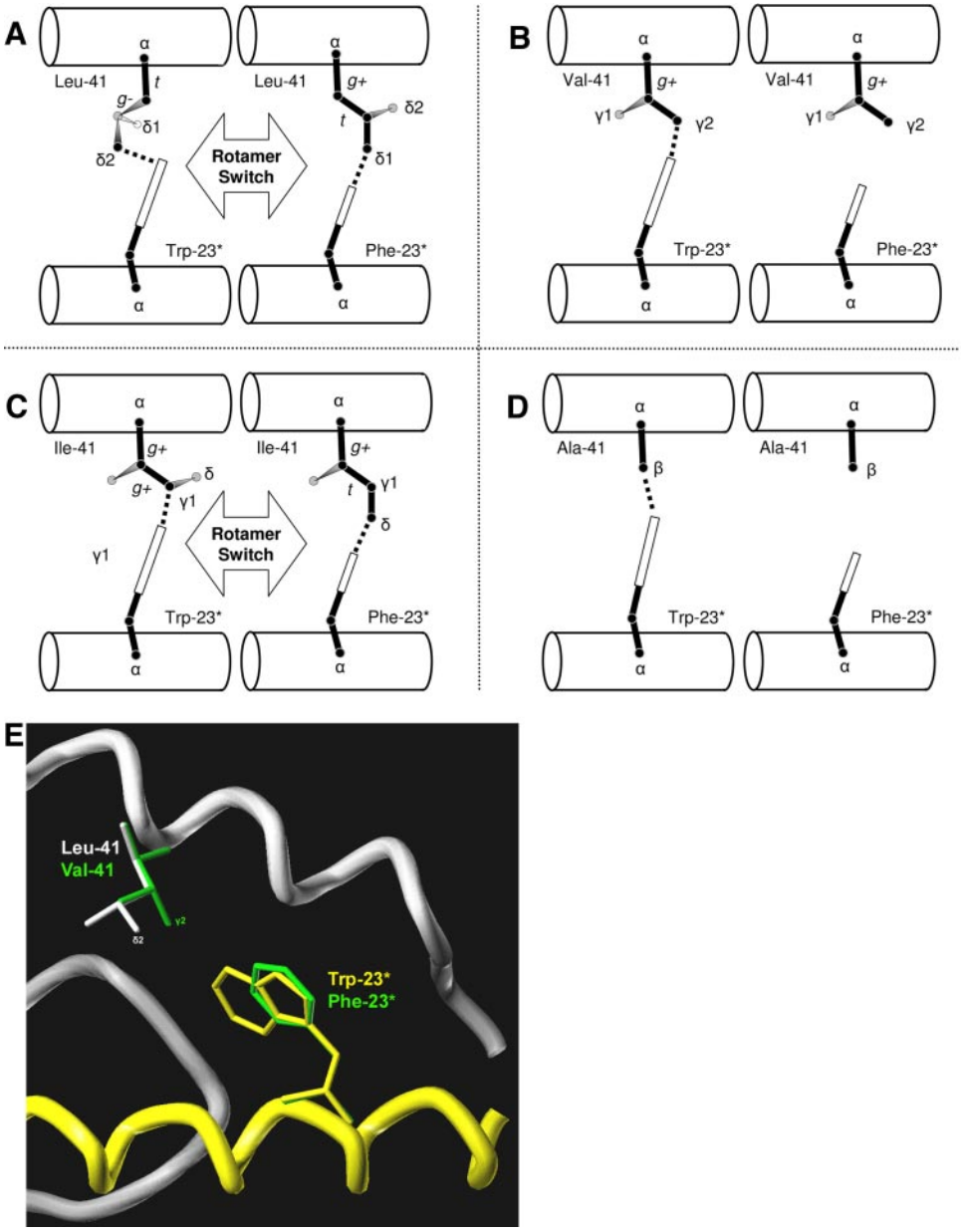

Fig. 6. A–D, diagrams based on the coordinates of the PTH/PTH-1R N domain crystal structure and seven of the nine final models derived from the in silico mutagenesis analysis. The nature of residue-41 is depicted in each panel with Leu-41 (A), Val-41 (B), Ile-41 (C), and Ala-41 (D) (the panels share the same arrangement as the binding data in Figs. 4 and 5). Left, interaction of residue 41 with Trp-23*; right, interaction of residue 41 with Phe-23*. The rotamers of the residue 41 side chains are shown as $g+ = gauche(+)$, $g- = gauche(-)$, and $t = trans$, and certain side-chain atom names are shown for clarity. To aid direct comparison among the rotamers of Leu, Ile, and Val, $\chi 1$ was measured to γ of Leu, $\gamma 1$ of Ile, and $\gamma 2$ of Val, whereas $\chi 2$ was measured to δ of Ile and $\delta 1$ of Leu. van der Waals interactions between the receptor and ligand, as defined by a distance of <3.8 Å, are depicted with a dashed line. Leu-41 and Ile-41 are able to interact with either Trp-23* or Phe-23* by toggling between two alternative rotamers (i.e., via a "rotamer switch"). Val-41 and Ala-41 are able to interact with Trp-23* but not with Phe-23*. E, part of the X-ray structure of PTH (yellow ribbon) bound to the N domain of PTH-1R (white ribbon) with the side chains of Trp-23* and Leu-41 highlighted. The nearest distance between the $\delta 2$ atom of Leu-41 and the indole ring is 3.5 Å. Superimposed upon the crystal structure are the in silico mutations of Leu-41 to Val and Trp-23* to Phe (both in green). Although the $\gamma 2$ atom of Val can interact with the indole ring of Trp-23* (3.2 Å), it cannot interact with the benzyl ring of Phe-23* (4.7 Å.).

data suggest that the highly conservative substitution of Leu-41 of PTH-1R for Val is sufficient to impart the ability to select PTH/PTHrP peptides.

To further understand the nature of this selectivity, Leu-41 in PTH-1R was substituted by Ile, Met, and Ala. Although the Met and Ile substitutions resulted in receptors that resembled the Leu-41 wild type receptor, the smaller side chains of Val and Ala resulted in a remarkable increase in Trp23/Phe23 selectivity (Table 3; Figs. 4 and 5). The data not only identified a receptor-ligand interaction site but also demonstrated that the nature of the Trp23/Phe23 selectivity filter was due to the size of the side chain of residue 41, with the smaller residues unable to optimally interact with Phe-23* of the ligand.

We have recently witnessed a great increase in our knowledge of how Family B GPCRs bind their ligands with the publication of several NMR and X-ray structures of ligand-receptor complexes (Grace et al., 2004, 2007; Parthier et al.,

2007; Sun et al., 2007; Runge et al., 2008). Of particular relevance to this work is the publication of the X-ray structure of PTH bound to the N domain of PTH-1R (Pioszak and Xu, 2008), which has enabled a rigorous analysis of our data within the context of a precise structure of the ligand-receptor complex. Shape-correlation statistics of the X-ray structure have demonstrated that the binding specificity of PTH to PTH-1R is largely determined by complementary shape-matching between hormone and receptor (Pioszak and Xu, 2008). Furthermore, it is also clear from the crystal structure that Trp-23* of PTH does indeed interact closely with Leu-41 (e.g., Fig. 6E), because there are two interactions of 3.5 to 3.7 Å between the Cδ2 atom of Leu-41 and the indole ring of Trp-23*. Moreover, this demonstrates that the mutagenesis/selectivity approach used in our analysis of this ligand-receptor interaction represented a highly successful strategy for identifying this precise and functionally relevant residue-residue contact.

Analysis of the X-ray structure and the nine in silico mutants indicated that Trp-23* on PTH was capable of forming an intimate van der Waals contact (defined as a carbon-carbon distance of ≤3.8 Å) with all of the mutated side chains at residue 41: Ile, Met, Val, and Ala (Fig. 6, A–D). However, the smaller side chain of Phe-23* was only able to contact the larger side chains of Leu, Met, and Ile but not the smaller side chains of Val and Ala (minimum distance possible was 4.7 Å or 5.4 Å, respectively). The data demonstrate that the Trp23/Phe23 selectivity filter is formed by the reduction of the volume of the side chain at position 41. It is noteworthy that before the publication of the PTH-1R/PTH crystal structure, we had come to precisely the same conclusion through building and analyzing a homology model of PTH bound to PTH-1R based upon the X-ray structure of the GIP/GIP receptor complex, demonstrating the usefulness of such models in the absence of an experimentally determined structure (Mann, 2007). However, the precision of the X-ray structure has enabled us to propose a more detailed mechanism for this remarkable and subtle selectivity filter.

We propose that the receptor species with Val or Ala at position 41 contain a crevice within the broader ligand binding groove that forms an intimate docking site for the side chain of Trp-23* but not for Phe-23* (Fig. 6, B and D). The lack of interaction with the smaller side chain of Phe-23* is the result of the small size of Val and Ala and the absence of a δ carbon atom. The resultant Trp23/Phe23 selectivity filter is eliminated in wild type PTH-1R by the presence of Leu-41, which has the conformational flexibility to switch between two different docking modes, each one optimal for either Trp-23* or Phe-23* (Fig. 6 A). In one docking mode, Leu-41 maintains the small crevice to allow room for the side chain of Trp-23* while still forming a van der Waals contact through its δ2 methyl group via the rotamer $\chi1 = trans$, $\chi2 = gauche(-)$ (Fig. 6A, left). Nevertheless, by adopting the more favored rotamer $\chi1 = gauche(+)$, $\chi2 = trans$ (Penel and Doig, 2001), Leu-41 can partly fill the crevice and enable an intimate contact between the δ1 methyl group and the smaller side chain of Phe-23* (Fig. 6A, right; note that this side chain rotamer would result in a steric clash between the δ1 methyl group and Trp-23*). Hence Leu-41 acts as a "rotamer toggle switch" enabling PTH-1R to adopt optimal docking sites for both Trp-23* and the Phe-23*.

In the case of the Ile-41 mutant, its β-branch means that the χ1 dihedral must be *gauche*(+) to avoid a steric clash with the main chain α-helix. With ligands that contain Phe-23*, a contact between the δ methyl group and the benzyl ring can only be formed via $\chi2 = trans$ (Fig. 6C, right) in a manner analogous to that of Leu-41 (Fig. 6A, right). However, this side-chain conformation cannot accommodate Trp-23* because of steric interference, and therefore the δ methyl group rotates out of the way by adopting $\chi2 = gauche(+)$ (Fig. 6C, left). Indeed this side-chain rotamer [$\chi1 = gauche(+)$, $\chi2 = gauche(+)$] is highly favored for Ile in α-helices (Penel and Doig, 2001). Therefore, like Leu-41 in PTH-1R, Ile-41 can also adopt the optimal docking sites for both Trp-23* and Phe-23* via a rotamer toggle mechanism. In a similar manner, the δ sulfur atom on Met can mimic the position of the δ2 carbon of Leu-41 when interacting with Trp-23* via $\chi1 = trans$, $\chi2 = trans$, whereas the Leu-41 to Phe-23* interaction can be mimicked via the more favored $\chi1 = gauche(+)$, $\chi2 = trans$ rotamer.

In summary, by transferring the Trp23/Phe23 selectivity filter from PTH-2R to PTH-1R, we have identified a functionally relevant interaction between residue 41 of the receptor and residue 23* of the ligand, which is compatible with the X-ray structure of the ligand-receptor complex. Furthermore, by substituting Leu-41 of PTH-1R with a range of similar hydrophobic amino acids, we have demonstrated that the size of the aliphatic side chain at residue 41 is the determining factor in the ability of the receptor to select between peptides with a either Trp or Phe at residue 23*. Moreover, a detailed in silico mutagenesis analysis of the N domain of PTH-1R bound with PTH demonstrated that it is the conformational flexibility of the larger aliphatic side chain of Leu (as well as Ile and Met), which enables it to accommodate both Trp-23* and Phe-23* in PTH-1R via a rotamer toggle mechanism that can switch between the two optimal docking conformations. The absence of such conformational flexibility when residue 41 is Val (or Ala) results in the creation of the Trp23/Phe23 selectivity filter.

Acknowledgments

We thank BBSRC and GlaxoSmithKline for funding.

References

Bergwitz C, Gardella TJ, Flannery MR, Potts JT Jr, Kronenberg HM, Goldring SR, and Jüppner H (1996) Full activation of chimeric receptors by hybrids between parathyroid hormone and calcitonin—evidence for a common pattern of ligand-receptor interaction. *J Biol Chem* **271:**26469–26472.

Bergwitz C, Jusseaume SA, Luck MD, Jüppner H, and Gardella TJ (1997) Residues in the membrane-spanning and extracellular loop regions of the parathyroid hormone (PTH)-2 receptor determine signaling selectivity for PTH and PTH-related peptide. *J Biol Chem* **272:**28861–28868.

Castro M, Nikolaev VO, Palm D, Lohse MJ, and Vilardaga JP (2005) Turn-on switch in parathyroid hormone receptor by a two-step parathyroid hormone binding mechanism. *Proc Natl Acad Sci U S A* **102:**16084–16089.

Dean T, Khatri A, Potetinova Z, Willick GE, and Gardella TJ (2006) Role of amino acid side chains in region 17–31 of parathyroid hormone (PTH) in binding to the PTH receptor. *J Biol Chem* **281:**32485–32495.

Gardella TJ, Luck MD, Jensen GS, Usdin TB, and Jüppner H (1996) Converting parathyroid hormone-related peptide (PTHrP) into a potent PTH-2 receptor agonist. *J Biol Chem* **271:**19888–19893.

Gensure RC, Gardella TJ, and Jüppner H (2001) Multiple sites of contact between the carboxyl-terminal binding domain of PTHrP-(1–36) analogs and the amino-terminal extracellular domain of the PTH/PTHrP receptor identified by photoaffinity cross-linking. *J Biol Chem* **276:**28650–28658.

Grace CR, Perrin MH, DiGruccio MR, Miller CL, Rivier JE, Vale WW, and Riek R (2004) NMR structure and peptide hormone binding site of the first extracellular domain of a type B1 G protein-coupled receptor. *Proc Natl Acad Sci U S A* **101:**12836–12841.

Grace CR, Perrin MH, Gulyas J, DiGruccio MR, Cantle JP, Rivier JE, Vale WW, and Riek R (2007) Structure of the N-terminal domain of a type B1 G protein-coupled receptor in complex with a peptide ligand. *Proc Natl Acad Sci U S A* **104:**4858–4863.

Hoare SR and Usdin TB (1999) Quantitative cell membrane-based radioligand assays for parathyroid hormone receptors. *J Pharmacol Toxicol* **41:**83–90.
Lanske B, Karaplis AC, Lee K, Luz A, Vortkamp A, Pirro A, Karperien M, Defize LH, Ho C, Mulligan RC, et al. (1996) PTH/PTHrP receptor in early development and Indian hedgehog-regulated bone growth. *Science* **273:**663–666.
López de Maturana R, Willshaw A, Kuntzsch A, Rudolph R, and Donnelly D (2003) The isolated N-terminal domain of the glucagon-like peptide-1 (GLP-1) receptor binds exendin peptides with much higher affinity than GLP-1. *J Biol Chem* **278:**10195–10200.
Mann RJ (2007) Selective peptide binding determinants on the N-terminal domain of parathyroid hormone receptors. PhD Thesis, University of Leeds, Leeds,UK.
Mannstadt M, Luck MD, Gardella TJ, and Jüppner H (1998) Evidence for a ligand interaction site at the amino-terminus of the parathyroid hormone (PTH)/PTH-related protein receptor from cross-linking and mutational studies. *J Biol Chem* **273:**16890–16896.
Parthier C, Kleinschmidt M, Neumann P, Rudolph R, Manhart S, Schlenzig D, Fanghänel J, Rahfeld JU, Demuth HU, and Stubbs MT (2007) Crystal structure of the incretin-bound extracellular domain of a G protein-coupled receptor. *Proc Natl Acad Sci U S A* **104:**13942–13947.
Penel S and Doig AJ (2001) Rotamer strain energy in protein helices - quantification of a major force opposing protein folding. *J Mol Biol* **305:**961–968.
Pham VI and Sexton PM (2004) Photoaffinity scanning in the mapping of the peptide receptor interface of class II G protein-coupled receptors. *J Pept Sci* **10:**179–203.
Pioszak AA and Xu HE (2008) Molecular recognition of parathyroid hormone by its G protein-coupled receptor. *Proc Natl Acad Sci U S A* **105:**5034–5039.
Runge S, Thøgersen H, Madsen K, Lau J, and Rudolph R (2008) Crystal structure of the ligand-bound glucagon-like peptide-1 receptor extracellular domain. *J Biol Chem* **283:**11340–11347.
Segre GV, Rosenblatt M, Reiner BL, Mahaffey JE, and Potts JT Jr (1979) Characterization of parathyroid-hormone receptors in canine renal cortical plasma-membranes using a radioiodinated sulfur-free hormone analog—correlation of binding with adenylate-cyclase activity. *J Biol Chem* **254:**6980–6986.
Sun C, Song D, Davis-Taber RA, Barrett LW, Scott VE, Richardson PL, Pereda-Lopez A, Uchic ME, Solomon LR, Lake MR, et al. (2007) Solution structure and mutational analysis of pituitary adenylate cyclase-activating polypeptide binding to the extracellular domain of PAC1-RS. *Proc Natl Acad Sci U S A* **104:**7875–7880.
Turner PR, Mefford S, Bambino T, and Nissenson RA (1998) Transmembrane residues together with the amino terminus limit the response of the parathyroid hormone (PTH) 2 receptor to PTH-related peptide. *J Biol Chem* **273:**3830–3837.
Usdin TB, Gruber C, and Bonner TI (1995) Identification and functional expression of a receptor selectively recognizing parathyroid hormone, the PTH2 receptor. *J Biol Chem* **270:**15455–15458.

Address correspondence to: Dr. Dan Donnelly, Institute of Membrane and Systems Biology, LIGHT Laboratories, Faculty of Biological Sciences, University of Leeds, Leeds LS2 9JT. E-mail: d.donnelly@leeds.ac.uk